Electronic Supplementary Material (ESI) for Journal of Materials Chemistry C.

Electronic Supporting Information

UV-Visible radiation modulation abilities of photon Up-Converting nanocapsules integrated with an oscillatory reaction

Giulia Quaglia [a], Beatrice Bartolomei [a], Pier Luigi Gentili [a] and Loredana Latterini [a]*

[a] Dipartimento di Chimica, Biologia e Biotecnologie - Università degli Studi di Perugia, via Elce di Sotto, 8, 06123 Perugia, Italy

E-mail: loredana.latterini@unipg.it

Content:

- Intensity of signals at 645 nm Vs irradiation time upon excitation at 360 nm (with oscillatory radiation) and 535 nm. page 8

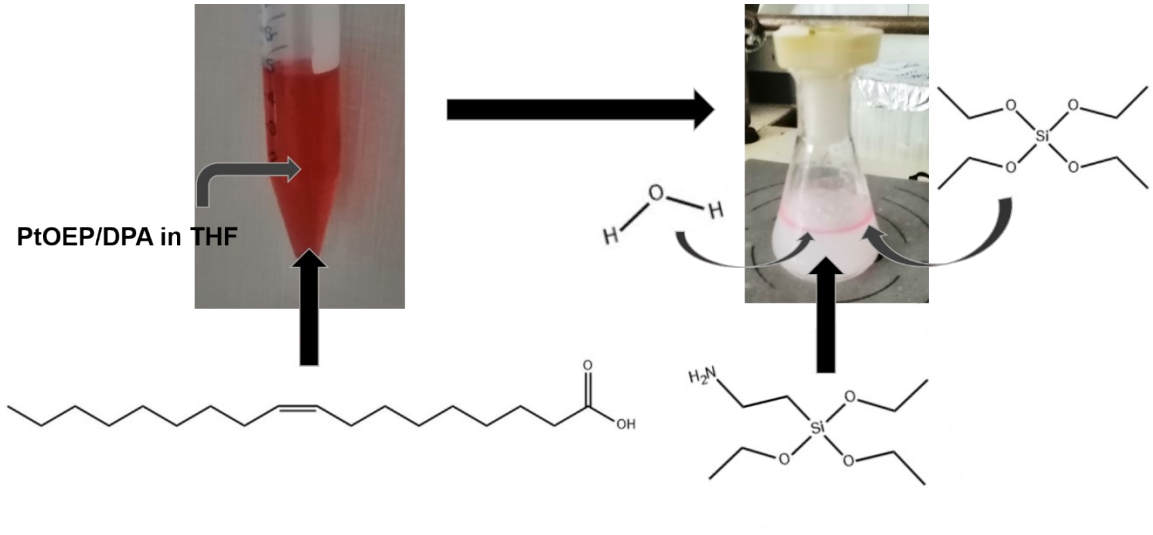

Scheme S1 UC-NC synthetic process.

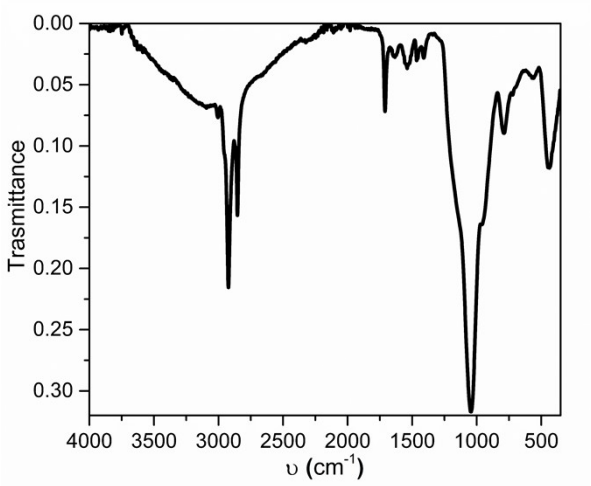

Figure S1 ATR-IR Spectrum of upconverting nanocapsules.

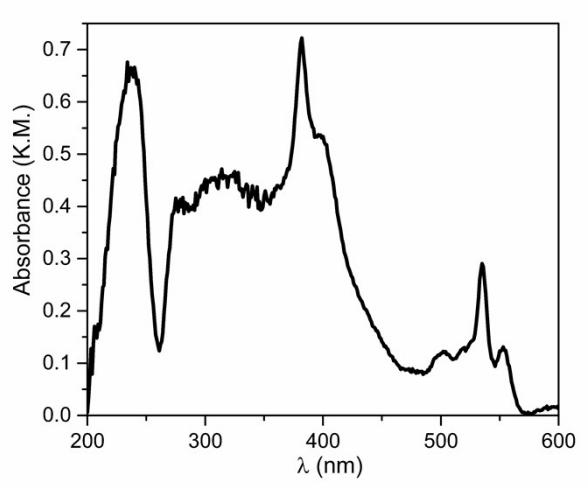

Figure S2 UV-Vis absorption spectrum (in Kubelka-Munk units) of upconverting nanocapsules.

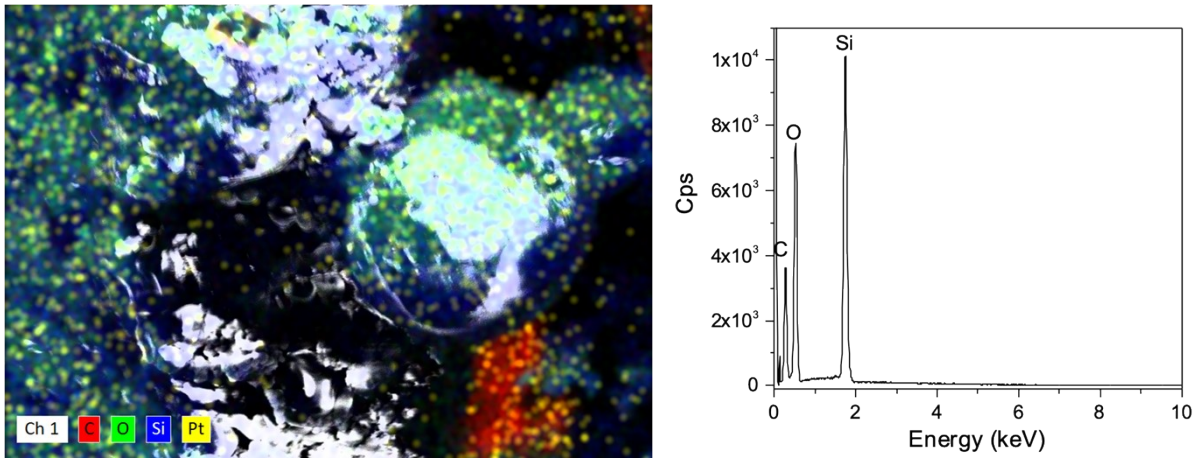

Figure S3. EDX mapping and spectra of upconverting nanocapsules.

Characterization of PtOEP/DPA in oleic acid solution

UC- emission spectrum of PtOEP/DPA in oleic acid has been measure and monitored as a function of the excitation power (Figure S3), generated by a 450 W xenon lamp. The sample was not previous deoxygenated.

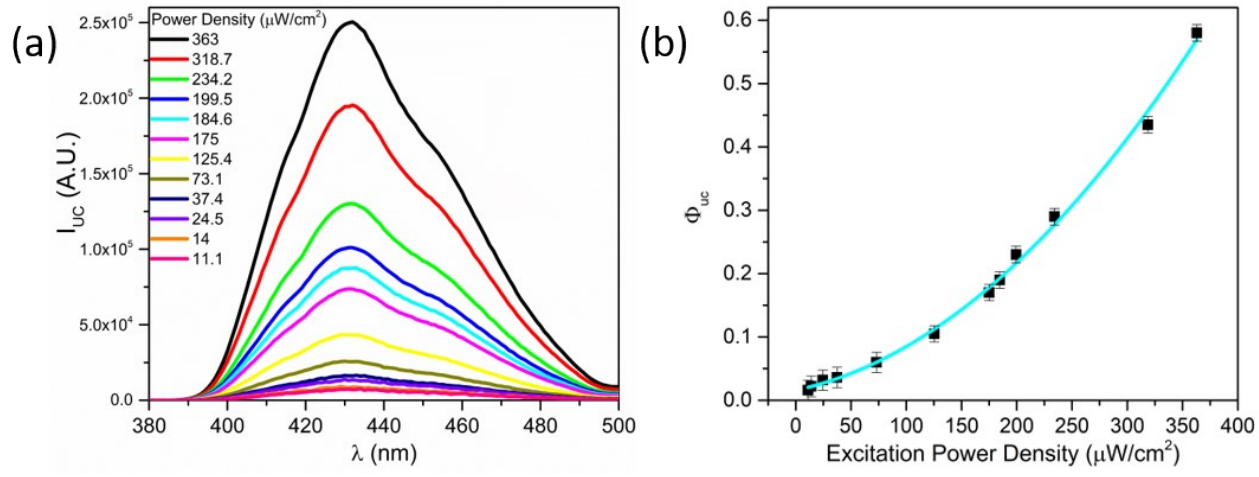

Figure S4 a) upconversion emission of PtOEP-DPA system in oleic acid solution. b) upconversion quantum yield vs excitation power density plot for PtOEP-DPA system in oleic acid solution.

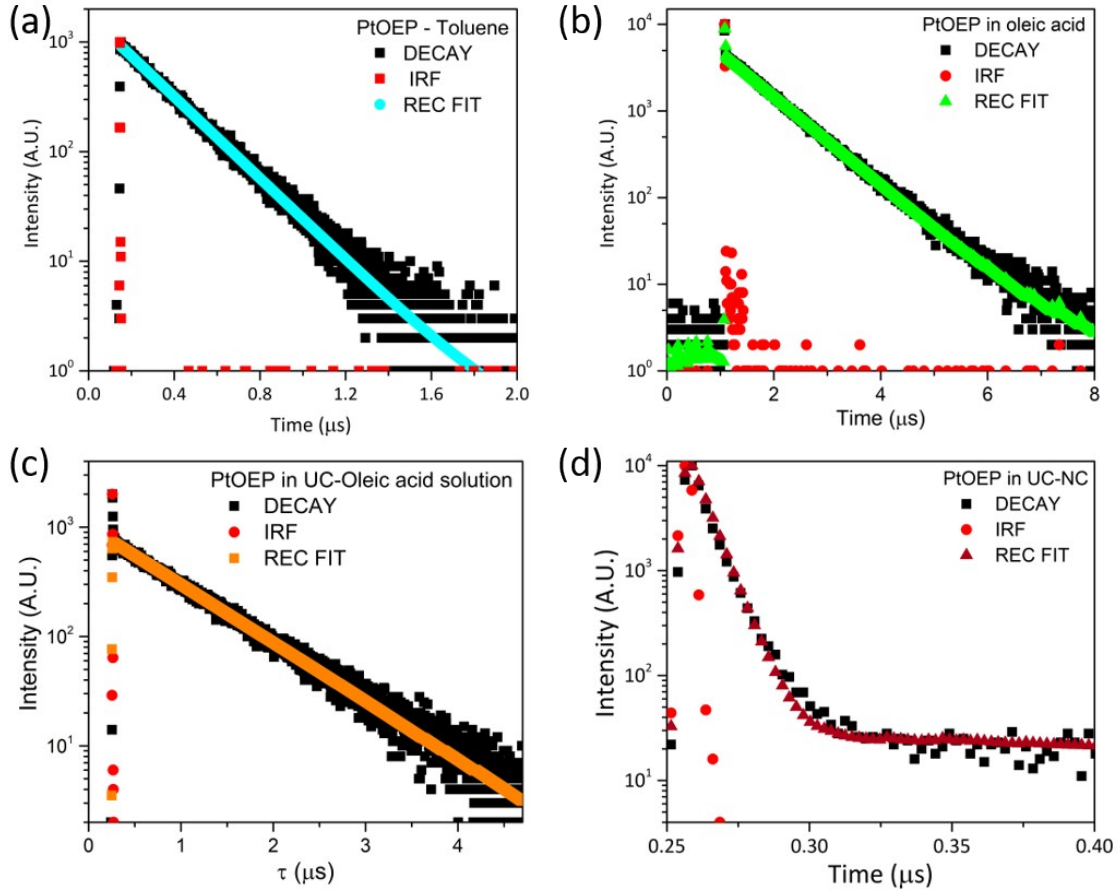

Figure S5 Phosphorescence decays of PtOEP in toluene (a), oleic acid (b); Phosphorescence decays of PtOEP in the presence of DPA in oleic acid solution (c) and in UC-NC solid-like powder (d) registered in aerated conditions.

Table S1 Luminescence decays parameters of PtOEP in toluene, oleic acid in the absence and in the presence of DPA and in UC-NC.

λ_{exc} - λ_{em} (nm)	Detected emission	Average Decay From MEM distributions
510 nm – 645 nm	PtOEP in toluene	τ_1 = 75.2 ns τ_2 = 235 ns
510 nm – 645 nm	PtOEP in OA solution	τ_1 = 410 ns τ_2 = 1.01 μs
510 nm – 645 nm	PtOEP in UC-OA solution (with DPA)	τ_1 = 2.35 ns τ_2 = 818.6 ns
510 nm – 645 nm	PtOEP in UC-NC (with DPA)	τ_1 = 1.8 ns τ_2 = 6.8 ns

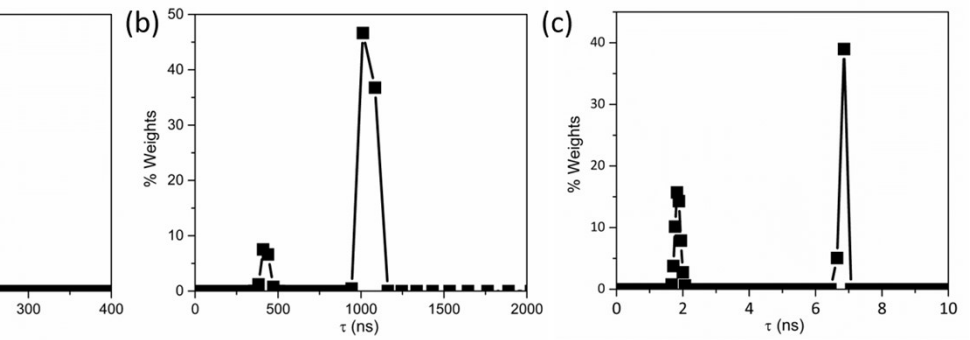

Figure S6 MEM analysis of PtOEP in toluene (a) and oleic acid (b) in absence of DPA and in solid-like powder UC-NC (c).

Table S2 Fuzzy Entropy (H) values determined for the different samples in different excitation conditions.

Sample	λ_{exc} (nm) [Excitation condition]	Fuzzy Entropy (H)
DPA in OA	[direct]	0.11
DPA in UC-NC	[direct]	0.29
PtOEP in Toluene	[direct]	0.19

PtOEP in OA	[direct]	0.21
PtOEP in UC-NC	[direct]	0.27
UC signal by DPA	[UC]	0.59

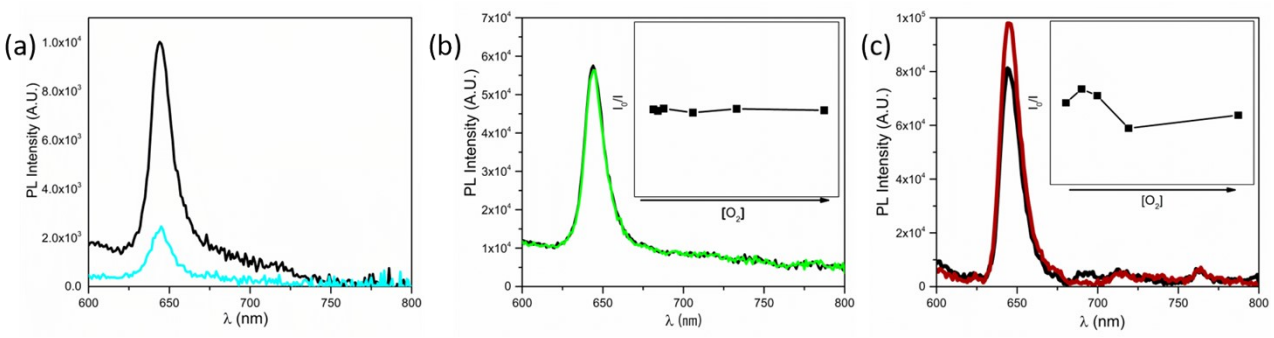

Figure S7 Phosphorescence spectra of PtOEP in toluene (A) and oleic acid (B) solution, and UC-NC (C) registered at different intervals of time of O_2 flow. Insert: Plot of I_0/I as a function of oxygen flow time.

Mechanism of the Belousov-Zhabotinsky (BZ) reaction

The BZ reaction is a catalysed oxidative bromination of malonic acid, which occurs according to the following equation:

$2BrO_3^-{}_{(aq)} + 3CH_2(COOH)_{2(aq)} + 2H^+_{(aq)} \rightarrow 2BrCH(COOH)_{2(aq)} + 3CO_{2(g)} + 4H_2O_{(l)}$

The mechanism of the BZ reaction, catalysed by cerium ions, consists of many elementary steps, which be grouped into three sets of chemical transformations:[1,2]

1) The first set consists in non-radical reactions, wherein the overall effect is the consumption of Br- and the production of $BrCH(COOH)_2$. This step is relevant when the concentration of Br- is high (above the critical value of 5×10^{-6}[BrO3-]) and the catalyst is in its reduced state (Ce(III)).
2) The second set of elementary steps consists in mono-electronic redox reactions, that occur when the Br^- concentration is driven below its critical value and the autocatalyst bromous acid becomes the main character. In this stage, Ce(IV) is produced.
3) To restore the Ce(III) state, a new set of reactions needs to occur: the bromomalonic acid is oxidized up to CO_2 and H_2O, consuming Ce(IV) and producing again Br^-. When [Br^-] becomes higher than its critical value (i.e., above 5×10^{-6}[BrO_3^-]), the first set of elementary steps restarts again.

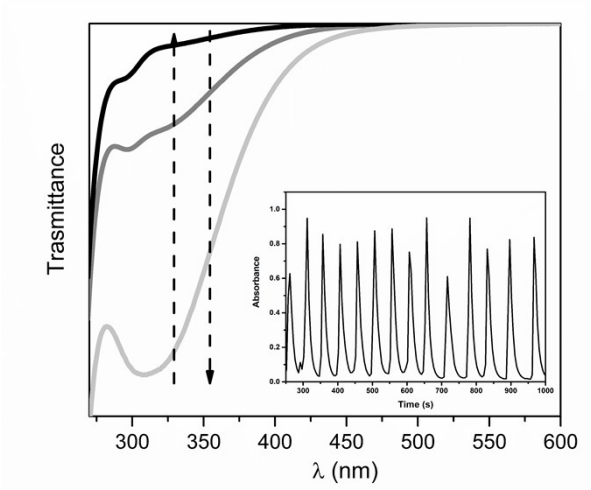

Figure S8 Transmittance evolution spectra and kinetic profile (insert) of the optical density of Belousov-Zhabotinsky solution.

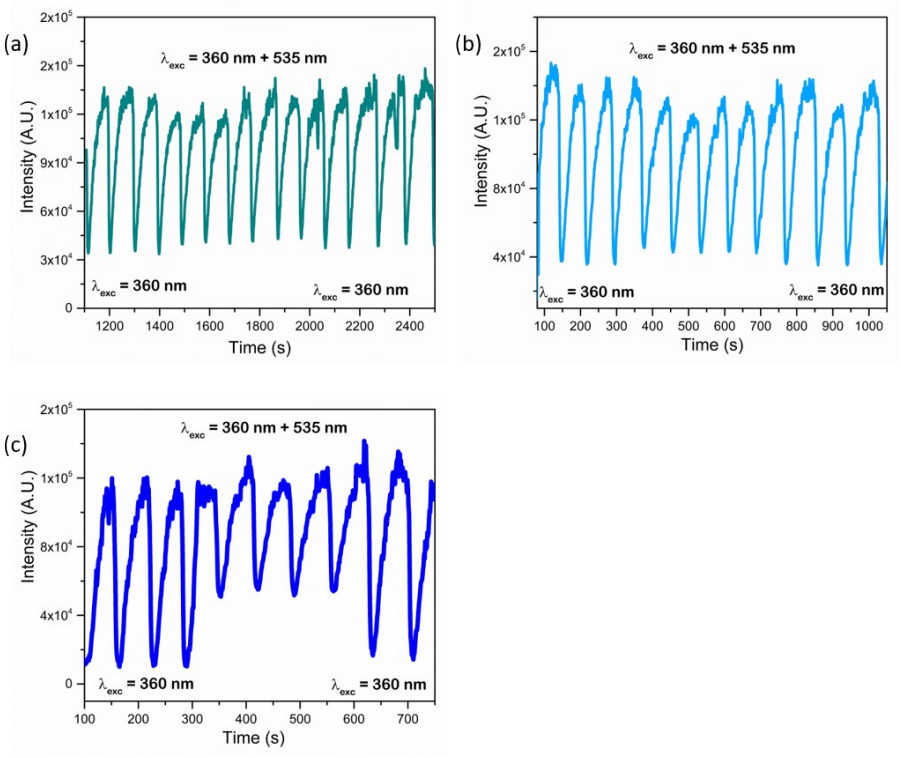

Figure S9 Intensity of signals at 430 nm Vs irradiation time upon excitation at 360 nm (0-1800 s) and 535 nm (between 600 s and 1200 s) with a power density of 55 μW/cm^2). Power density at 360 nm of 13 (A) 6 (B) 1 (C) μW/cm^2.

Table S3 Amplitude variation of the output signal of DPA in presence of a double excitation (360 nm + 535 nm), referred to the amplitude of the same signal obtained with a single input (360 nm).

360 nm Power excitation (μW/cm^2)	Δ-Amplitude ($I_{360\ nm}$ -$I_{360\ nm\ +\ 535\ nm}$)/$I_{360\ nm}$
13	0.08
6	0.13
1	0.37

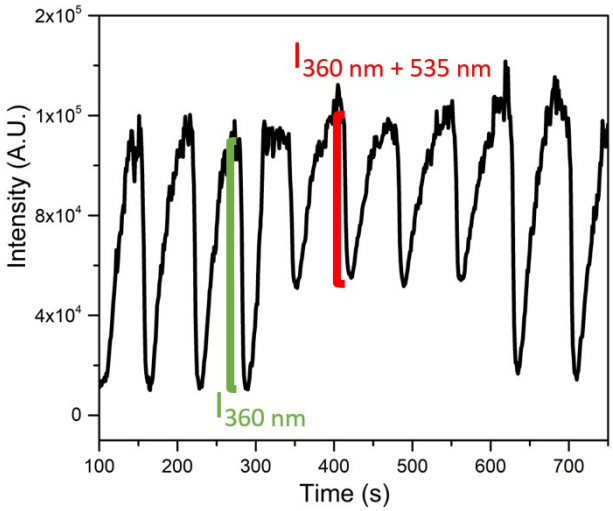

Scheme S2 Amplitude of the output signal of DPA in presence of single (360 nm, in green) and simultaneous excitation (360 nm plus 535 nm, in red).

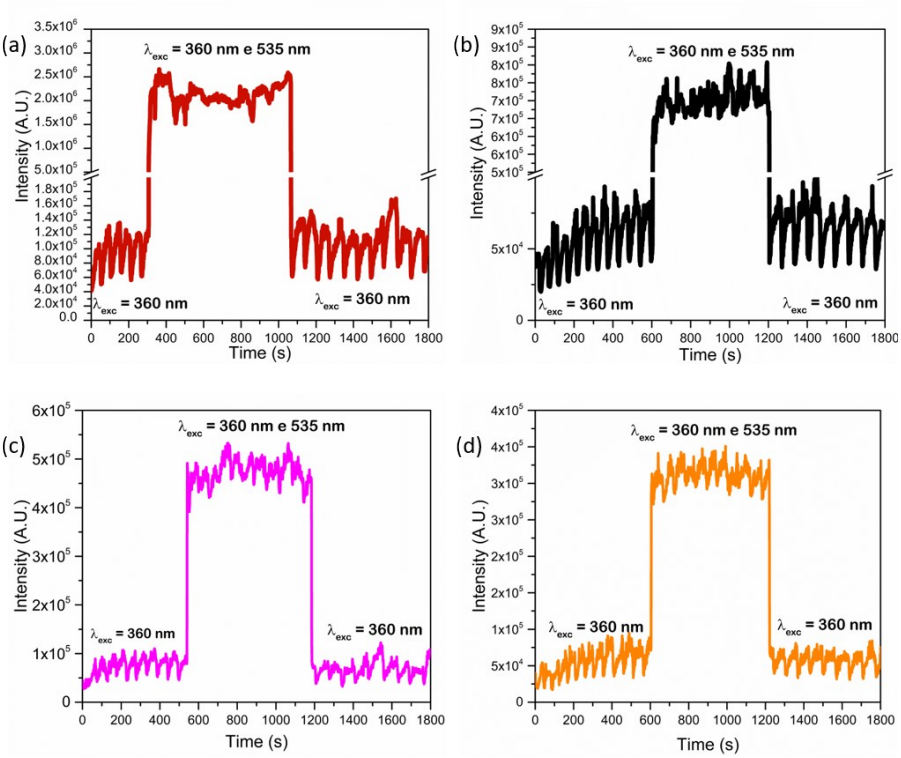

Figure S10 Intensity of signals at 645 nm Vs irradiation time upon excitation at 360 nm (0-1800 s) and 535 nm (between 600 s and 1200 s) with a power density 133µW/cm^2; power density at 535 nm of 55 µW/cm^2 (A), 11 µW/cm^2 (B) 5.5 µW/cm^2 (C) 2.8 µW/cm^2 (D).

References

1 P.L. Gentili and J.C. Micheau, *J. of Photochem. Photobiol. C*, 2020, **43**, 10032.

2 R. J. Field, E. Koros and R. M. Noyes*, J. Am. Chem. Soc*., 1972, **94**, 8649–8664.

3 C. Clementi, B. Doherty, P.L. Gentili, C. Miliani, A. Romani, B.G. Brunetti, A. Sgamellotti, *Appl. Phys. A*, 2008, **92**, 25-33.